Biochemistry

 Volume 41, Number 30 July 30, 2002

Current Topics

Catalytic Mechanism of the Topa Quinone Containing Copper Amine Oxidases†

Minae Mure,‡ Stephen A. Mills,‡ and Judith P. Klinman*,§

Department of Chemistry, University of California, Berkeley, California 94720

Received March 27, 2002; Revised Manuscript Received May 23, 2002

The discovery of 2,4,5-trihydoxyphenylalanine quinone, or topaquinone [TPQ (*1*)][1] in copper amine oxidases (CAOs) defined a new class of enzymatic redox cofactors derived from the post-translational modification of tyrosine or tryptophan protein side chains to form quinonoid structures. Figure 1A shows the structures of the cofactors which have been characterized, namely, TPQ, lysine tyrosyl quinone [LTQ, formed via the cross-linking of a tyrosine and a lysine side chain (*2*)], tryptophan tryptophyl quinone [TTQ, formed via the cross-linking of two tryptophan side chains (*3*)], and cysteine tryptophyl quinone [CTQ, formed via the cross-linking of a cysteine and a tryptophan side chain (*4*)]. It has been shown that TPQ formation in CAOs proceeds through a copper-ion-dependent autoxidation which does not require another enzyme (*5*, *6*). The details of the mechanism of TPQ biogenesis are less well established than those for catalytic turnover and are an active area of investigation (cf. refs *7* and *8*). In the present review, we focus on the increasingly well-described role for TPQ in the conversion of the substrates, primary amines and molecular oxygen, to aldehydes and hydrogen peroxide, respectively. Since the kinetics of the TPQ enzymes display a classical ping pong mechanism (*9*), it is relatively easy to examine each of the half reactions involving substrate amine oxidation (reductive half reaction, eq 1) and dioxygen reduction (oxidative half reaction, eq 2):

$$E_{ox} + RCH_2NH_3^+ \rightleftharpoons E_{ox}{-}RCH_2NH_3^+ \rightarrow E_{red} + RCHO + H_2O$$

$$E_{red} + O_2 + H_2O \rightarrow E_{ox} + NH_4^+ + H_2O_2$$

REDUCTIVE HALF REACTION (k_{cat}/K_m FOR AMINE)

In the reductive half reaction, CAOs catalyze the conversion of an aliphatic or aromatic primary amine to an aldehyde, which results in the reduction of TPQ to an aminoquinol form. This first half reaction has been well characterized for a number of CAOs (*9*), providing solid evidence for the aminotransferase mechanism presented in Scheme 1. As illustrated, TPQ undergoes reduction by two electrons, thereby serving as a "storage site" for reducing equivalents that are ultimately transferred to molecular oxygen in the formation of hydrogen peroxide (see Oxidative Half Reaction below). The intermediates in Scheme 1 have been characterized by a combination of chemical, kinetic and spectroscopic means.

*Resting Form of CAO (**1** in Scheme 1).* Prior to their reaction with amines, CAOs show a characteristic broad absorption band with a λ_{max} at around 480 nm, arising from the oxidized form of TPQ (TPQ_{ox}) and resulting in their

† Supported by grants from the NIH (GM39296 to J.P.K.) and (GM08352 to S.A.M.).

* To whom correspondence should be addressed. Tel: 510-642-2668. Fax: 510-643-6232. E-mail: klinman@socrates.berkeley.edu.

‡ Both of these authors contributed equally.

§ J.P.K. is also in the Department of Molecular and Cell Biology.

[1] Abbreviations: CAO, copper containing amine oxidase; AGAO, *Arthrobacter globiformis* amine oxidase; BSAO, bovine serum amine oxidase; ECAO, *Escherichia coli* amine oxidase; HPAO, *Hansenula polymorpha* amine oxidase; WT-HPAO, wild-type HPAO; Co−HPAO, Co(II)-substituted HPAO; PSAO, pea seedling amine oxidase; PPAO, *Pichia pastoris* amine oxidase; TPQ, 2,4,5-trihydroxyphenylalanyl quinone, or topaquinone; TPQ_{ox}, oxidized form of TPQ; TPQ_{red}, reduced form of TPQ; TPQ_{sq}, semiquinone form of TPQ; TTQ, tryptophan tryptophyl quinone; CTQ, cysteine tryptophyl quinone; LTQ, lysine tyrosyl quinone; NHE, normal hydrogen electrode; TMPA, tris (2-pyridylmethyl) amine.

10.1021/bi020246b CCC: $22.00
Published on Web 06/25/2002

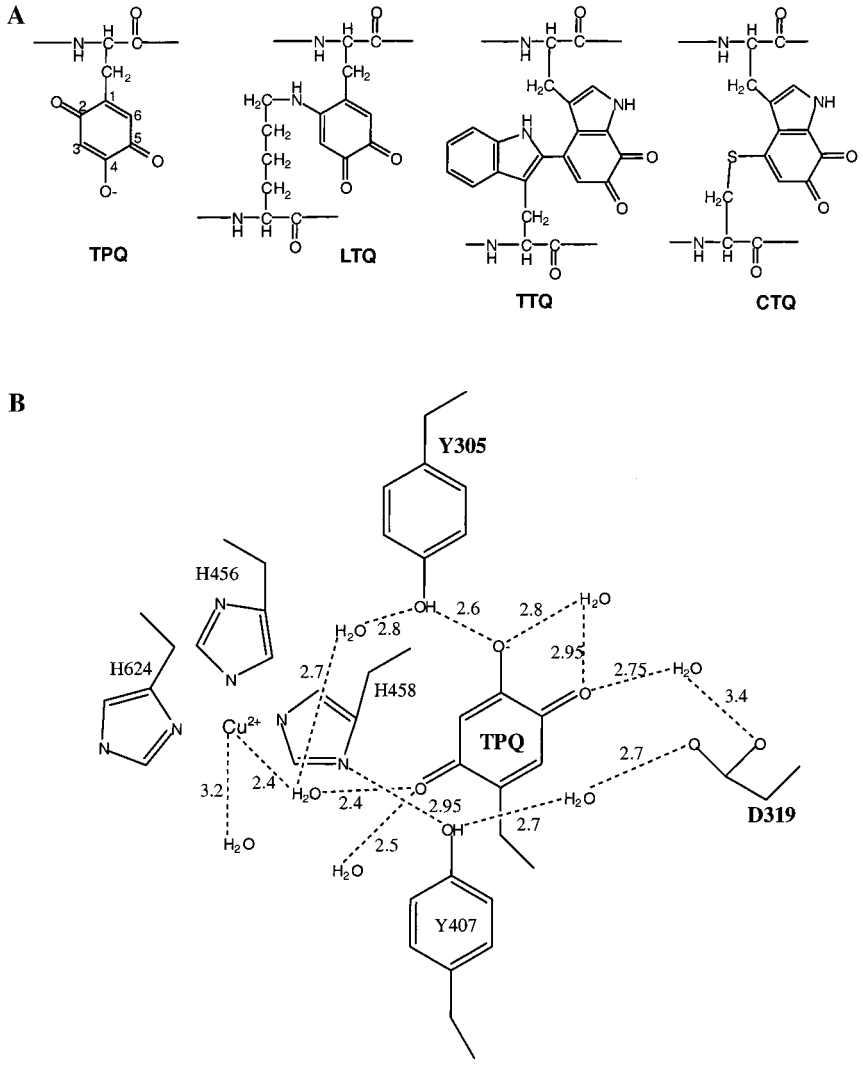

FIGURE 1: (A) Structure of protein-derived quinonoid cofactors. TPQ, 2,4,5-trihydroxyphenylalanyl quinone, or topaquinone; TTQ, tryptophan tryptophyl quinone; CTQ, cysteine tryptophyl quinone; LTQ, lysine tyrosyl quinone. (B) Schematic of key residues in the active site of HPAO. Hydrogen bonding interactions are shown with dotted lines, and the distances are in Å.

Table 1: Absorption Maxima of CAOs

enzyme source	λ_{max} (nm)	ϵ ($M^{-1}\,cm^{-1}$)
bovine serum (BSAO)	476	1900 (*50*)
pea seedling (PSAO)	500	2450 (*64*)
H. polymorpha (HPAO)	472	2400 (*65*)
P. pastoris (PPAO)	480	2070 (*63*)
E. coli (ECAO)	474	1990 (*14*)
A. globiformis (phenethylamine) (AGAO)	475	1700 (*11*)
A. globiformis (histamine)	498	1900 (*62*)
TPQ model (pH 2)	388	700 (*10*)
TPQ model (pH 7)	488	1800 (*10*)
TPQ model (in acetonitrile)	372	700 (*13*)
TPQ model (in acetonitrile + *tert*-butylamine)	498	2100 (*13*)

distinctive pink color. Depending on the source of CAO, the λ_{max} can vary from 472 to 500 nm (Table 1). TPQ_{ox} exists as an oxoanion due to the acidity of the 4-hydroxyl group [pK_a = 4.1 in a model compound (*10*) and ca. 3 in BSAO (*10*) and AGAO (*11*)]. Comparison of the resonance Raman spectra of the resting form of CAOs with a TPQ_{ox} model compound shows extensive delocalization of charge between the oxygens on C-2 and C-4 (*12*). A fully delocalized TPQ_{ox} model compound has a λ_{max} at 498 nm in anhydrous aprotic solvents, which shifts to 372 nm upon protonation (*13*). In aqueous solution, the model compound shows a λ_{max} at 488 nm, which shifts to 380 nm upon acidification (*10*). The differences in the λ_{max} among the CAOs are believed to reflect variations in the extent of the charge delocalization of TPQ_{ox} within the active site. The X-ray crystal structures of HPAO and ECAO show a highly conserved axial water molecule of the active site cupric ion and a strictly conserved Tyr (Y305 in HPAO, Y369 in ECAO), which form hydrogen bonds with the oxygens on C-2 and C-4, respectively (*14*, *15*) (Figure 1B). The latter is a relatively short hydrogen bond (2.6 Å in HPAO, 2.7 Å in ECAO), suggesting that this interaction is strong in these enzymes and may control the extent of charge localization at C-4. Elimination of the interaction by mutation of Tyr to Ala in HPAO (*16*) or Phe in ECAO (*14*) results in about a 15 nm red shift of the λ_{max} of TPQ_{ox}. However, the rate of enzymatic turnover with alipathic amines is practically unaltered (*14*, *16*).

The anionic form of TPQ_{ox} is resonance stabilized with reduced electrophilicity at the C-2 and the C-4 positions, which directs nucleophilic addition of an amine exclusively to the C-5 position (*13*, *17*) (cf. next section). Clearly, TPQ must be in a specific orientation to expose the C-5 to the substrate-binding site. There are a number of active site

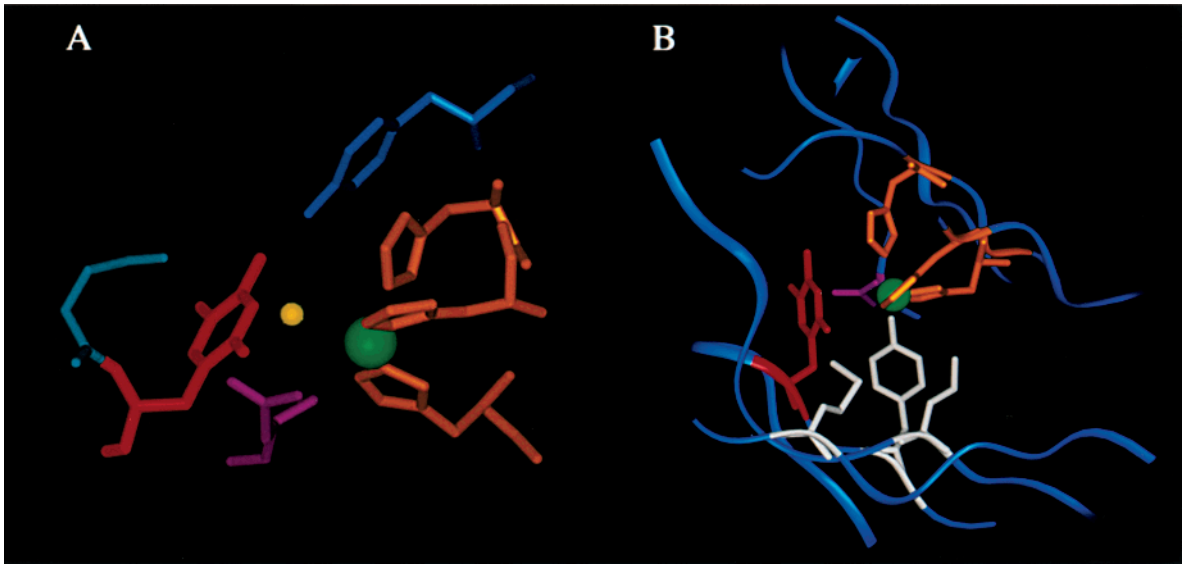

FIGURE 2: (A) Active site structure of HPAO showing residues important to orient TPQ for optimal catalysis. TPQ (in red), Y305 (in blue), D319 (in purple), N404 (in light blue), H458, H456, H624 (in orange), Cu^{2+} (in light green), and the axial water ligand to Cu^{2+} (in yellow) are highlighted. (B) Putative O_2 binding site of HPAO. The proposed hydrophobic pocket is composed of Y407, M634, and L425 (all shown in white). TPQ (in red), D319 (in purple), H458, H456, H624 (in orange), and Cu^{2+} (in light green) are also highlighted.

Scheme 1: Mechanism for the Reductive Half Reaction of CAOs

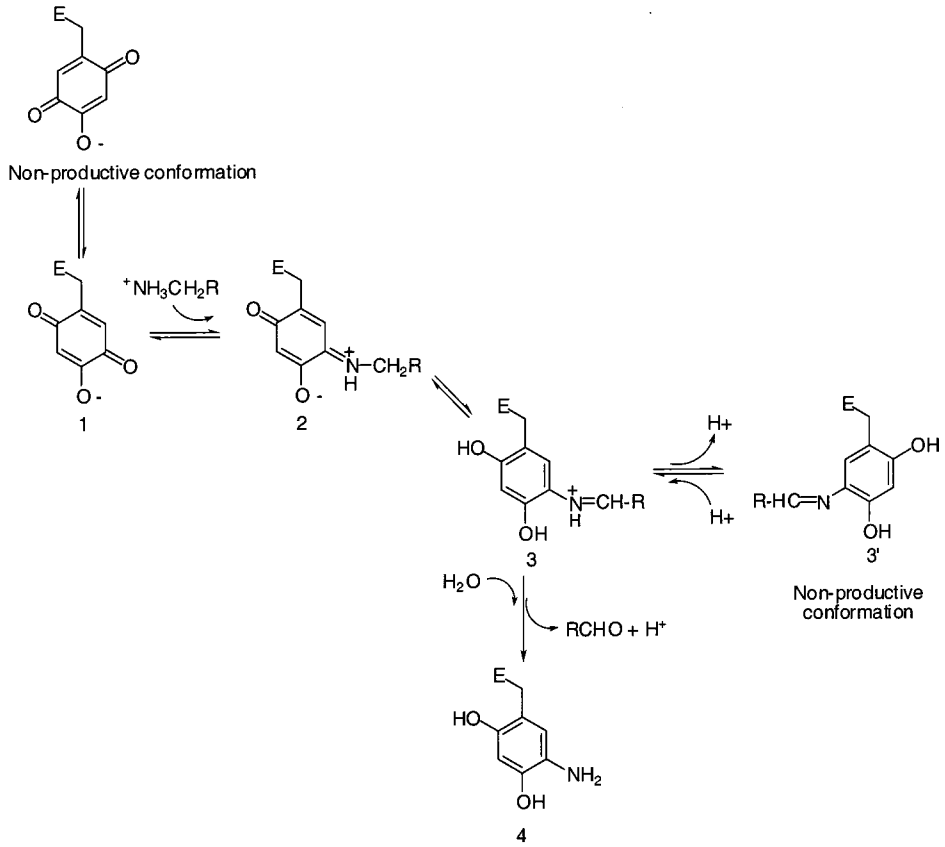

residues that have been implicated in controlling this orientation, shown in Figures 1B and 2A. One line of evidence for the dynamic nature of TPQ comes from isotope-labeling studies. Both the C-5 oxygen and C-3 proton of TPQ_{ox} analogues undergo exchange with O-18 water and D_2O, respectively (*12*). In wild-type HPAO, the C-5 oxygen of TPQ_{ox} rapidly exchanges with solvent water, whereas the C-3 proton is nonexchanging. This has been interpreted in terms of the relative solvent accessibility of these ring positions (*18*). In contrast to the wild-type, the mutants D319E (low activity) and D319N (inactive) show the reverse exchange pattern (*19*). Further, the mutant N404A (low activity) shows rapid exchange at both positions (*20*). These results can be explained if TPQ exhibits conformational mobility where, in the wild-type, most of the TPQ_{ox} is doriented in the catalytically active conformation, and in D319E and D319N, this is reversed. In the X-ray crystal structures of CAOs, TPQ_{ox} has been seen in different orientations, depending on the conditions under which the crystals were grown and the form of CAO and active site

mutant studied (*14*, *15*, *21*−*24*). In some cases, TPQ_{ox} is actually disordered. Recent solution studies of exchange by resonance Raman spectroscopy show good correlation with results from X-ray crystallography (*25*). It should be noted that the X-ray crystal structure of ECAO in which the active site base, an aspartate residue, has been converted to a glutamate residue (corresponding to D319E in HPAO) shows TPQ_{ox} in a productive orientation (analogous to WT); the exchange studies carried out on D319E of HPAO have yet to be repeated on this mutant form of ECAO.

For WT-HPAO and its D319E mutant form, NH_4^+ as well as other cations incapable of covalent addition to TPQ_{ox} (such as cesium and dimethylammonium ions) cause a substantial blue shift in the λ_{max} to around 345 nm at pH 9 (*19*). These results indicate that the blue shift does not arise from covalent addition of ammonia to TPQ_{ox} but, rather, is produced by binding of the cations in the vicinity of TPQ_{ox}. The fact that this species forms most readily at pH 9 suggests that the ionization of the active site base (D319) helps cation binding. In fact, cations have no effect on the D319N mutant (*19*). It has been proposed that these cations interact with the C-4 oxoanion of TPQ_{ox}, thereby causing the blue shift in the absorption of TPQ_{ox} (*19*); however, the extinction coefficient value of the species (2300−6700 M^{-1} cm^{-1}) is much larger than that obtained for the charge localized TPQ_{ox} (700 M^{-1} cm^{-1}) (Table 1). Interestingly, the structures of ECAO and AGAO obtained from colorless crystals grown in 2.3 M ammonium sulfate at pH 7−8.3 show TPQ_{ox} bound to the active site copper through the C-4 oxygen, although no ammonium ions were identified in the active sites (*21*, *23*). It is conceivable that the reported spectroscopic data for HPAO in the presence of monovalent cations reflect an inner sphere complex between the active site copper and TPQ_{ox}.

*Substrate Schiff Base Intermediate (**2** in Scheme 1).* A channel for amine substrate binding has been identified from X-ray crystallographic studies (*15*, *23*). The substrate binds to the active site in its protonated form and must be deprotonated to facilitate the nucleophilic addition to TPQ_{ox} (*9*). This deprotonation is most likely effected by the active site base. Covalent adduct formation is known to take place at the C-5 carbonyl group of TPQ_{ox}, as inferred from the reaction of CAOs and model compounds with inhibitors and substrate analogues (*17*, *26*) and from isotope exchange of the oxygen at C-5 observed by resonance Raman spectroscopy (*12*, *18*, *27*). The reaction between the substrate amine and the C-5 carbonyl group of TPQ_{ox} forms the first stable intermediate, the substrate Schiff base species (**2** in Scheme 1). Formation of **2** is expected to proceed via initial formation of a carbinolamine which then loses water, presumably by taking up a proton from the protonated active site base. However, the carbinolamine has thus far not been observed. The intermediacy of the substrate Schiff base species has been further implicated by chemical trapping experiments on BSAO (*28*) and Arthrobacter P1 amine oxidase (*29*). Rapid-scanning stopped-flow experiments with BSAO under anaerobic conditions indicated a transient species with a λ_{max} at 340 nm in the oxidation of benzylamine. The species with a λ_{max} at 340 nm was proposed to be a substrate Schiff base complex stabilized by a strong electrostatic interaction between the protonated imine nitrogen at C-5 and the C-4 oxoanion of TPQ. This assignment is supported by TPQ model compounds (*17*) where the C-4 oxoanion of substrate Schiff base compounds is localized by electrostatic interaction, maintaining the anionic electron density primarily on the C-4 oxygen to yield a λ_{max} at 340−350 nm. The delocalization of the charge results in a shift of the λ_{max} to 454 nm.

At the enzyme active site, there are two possible interactions that may be responsible for charge localization at the C-4 oxygen: a hydrogen-bonding interaction between the C-4 oxoanion of TPQ and the nitrogen of the protonated Schiff base at C-5 or a hydrogen-bonding interaction between the C-4 oxoanion of TPQ and an active site residue. The X-ray crystal structure of the ECAO-2-hydrazino pyridine complex provided the first direct observation of a substrate Schiff base-like species in the enzyme active site, where the distance between the C-4 oxygen and Y369 is shorter than that observed in the resting enzyme (2.4 Å versus 2.7 Å), implying a strengthening of this interaction (*26*).

The positive charge on the protonated Schiff base nitrogen at C-5 is also close to the active site base. Studies of the pH dependence of the reductive half reaction for BSAO (*30*) and HPAO (*16*) have implicated an elevated pK_a for the active site base in the resting form of the enzyme (pK_a ∼ 8), presumably due to charge repulsion with the anionic form of TPQ_{ox}, together with a reduced pK_a of 5−6 in the substrate Schiff base complex (see below). Thus, the charge on the protonated nitrogen at C-5 of the substrate Schiff base is expected to be stabilized by interactions involving both the deprotonated active site base and the C-4 oxoanion of TPQ.

*Product Schiff Base Intermediate (**3** in Scheme 1).* The conversion of the substrate Schiff base (**2** in Scheme 1) to the product Schiff base (**3** in Scheme 1) occurs via base-catalyzed abstraction of a proton at the C-1 position of the substrate in a step that is sensitive to deuterium or tritium labeling of the substrate (*30*, *31*). In the case of BSAO, the large size of the measured kinetic isotope effect on k_{cat}/K_m for benzylamine and their nonclassical temperature dependence have been used to implicate hydrogen tunneling in the C−H cleavage step (*32*). Detailed kinetic studies of the pH dependence of substrate oxidation by BSAO support the participation of a catalytic residue with pK_a of 5.6 (*30*). X-ray crystallographic studies on the active form structures of CAOs reveal a strictly conserved aspartate group (D319 for HPAO in Figures 1B and 2A) close to the C-5 position of the cofactor. The structure of the inhibited ECAO-2-hydrazino pyridine complex shows that this Asp is in an ideal position to act as the catalytic base (*24*). The mutation of the Asp to Asn completely eliminates the catalytic activity of HPAO (*19*) and ECAO (*24*), but if Asp is mutated to Glu, there is some activity, albeit less than with the wild type. The reduced activity of the Glu mutant in solution could be explained if most of the TPQ_{ox} is in a nonproductive orientation, due to steric repulsion between the longer side chain of Glu and the TPQ_{ox} (*19*).

In contrast to the substrate Schiff base (**2**), the product Schiff base (**3**) has never been directly detected under the normal catalytic turnover conditions (*28*, *29*). This is expected from the large hydrogen kinetic isotope effect on k_{cat}/K_m (amine) and the implication of the accumulation of the substrate Schiff base, together with model chemistry, which predicts the high reactivity of the product Schiff base toward hydrolysis (*17*). Formation of **3** has been inferred from tritium exchange experiments using a β-phenethylamine

labeled at the C-2 position, where the label was lost during turnover (*30*). This result indicates enamine formation from **3**, in which the C-2 protons would be acidic and undergo exchange with solvent. Further, a spectral intermediate, believed to be a delocalized form of **3**, was observed in a stopped-flow spectroscopic study using *para*-hydroxybenzylamine as a substrate (*33*).

In active site mutant forms of HPAO, such as E406N (*34*) and N404A (*20*) where these residues flank TPQ, a species with a λ_{max} at 380 nm accumulates in the steady-state reaction with methylamine as the substrate. Resonance Raman spectra of the 380 nm species indicate it is the neutral form of the product Schiff base (**3′** in Scheme 1). This absorbing species is believed to arise from rotation of the protonated Schiff base away from the active site base (analogous to that seen in the resting form of TPQ) leading to deprotonation and inhibition of hydrolysis. At low pH (<7), this species disappears, supporting the hypothesis that this Schiff base can be reprotonated (**3**), undergoing facile hydrolysis to yield the reduced TPQ (TPQ_{red}) in the aminoquinol form (**4** in Scheme 1) and a corresponding product aldehyde. The formation of a similar species with a λ_{max} at 388 nm was observed in Y305 mutants (Y305A or Y305F) (*16*). In contrast to the E406N and N404A intermediate, this species has a much shorter lifetime and rapidly disappears above pH 7.

The formation of the product Schiff base involves the formal transfer of two electrons from the substrate amine to TPQ_{ox}. Additionally, the oxygens at the C-2 and C-4 positions of TPQ are expected to be protonated as the pK_as of these positions increase upon reduction of the TPQ ring (*10*) (see below). The proton at the C-4 oxygen has been proposed to originate from the C-1 carbon of the substrate via the protonated active site base, regenerating D319 as an anion hydrogen bonded to the protonated imine nitrogen at C-5 (*9*). This protonation state of the active site base has been inferred from isotope exchange studies with BSAO where the radiolabel was lost from the C-2 position of tritiated phenethylamine substrates (*30*). Protonation of the C-4 oxygen is certainly one cause of the reduced stability of the product Schiff base intermediate that arises from a loss of electrostatic stabilization by the neighboring oxoanion (*9*, *17*).

The origin of the proton on the C-2 oxygen is less well understood and may derive from one of the copper bound waters. X-ray structural analyses of CAOs containing either oxidized (*15*, *21*, *23*, *35*) or reduced (*35*) forms of TPQ indicate that the axial water on copper is close to the C-2 oxygen of TPQ. In the reductive half reaction, it is assumed that protonation of the C-2 oxygen follows, rather than precedes, TPQ reduction to give TPQ_{red} in the neutral aminoquinol form along with copper hydroxide (*9*). This is because the C-4 oxygen of the substrate Schiff base intermediate is likely to be deprotonated (cf. pK_a = 3 for TPQ_{ox} in BSAO). Further, the significantly blue-shifted λ_{max} of the substrate Schiff base relative to TPQ_{ox} indicates charge localization at the C-4 oxygen while the C-2 oxygen remains neutral (see above). The higher pK_a for metal-bound water (estimated as 6−7 from the kinetics of the oxidative half reaction, see below) relative to TPQ_{ox} predicts a very low concentration of a protonated TPQ_{ox}, copper hydroxide intermediate that could be formed in a preequilibrium step. Only if such prior protonation confers exceptional reactivity, as suggested recently from density functional calculations (*36*), would proton transfer to the C-2 oxygen be expected to precede loss of proton from the C-1 position of substrate.

*Aminoquinol (**4** in Scheme 1).* The properties of the aminoquinol have been studied via the synthesis and characterization of model compounds (*10*) and through studies of substrate reduced forms of CAOs in the absence of O_2 (*33*, *37*). Model compounds for the aminoquinol indicate a λ_{max} of 310 nm at neutral pH and a redox potential of 0.11 V versus NHE, pH 6.8, as compared to the quinol derived from the reduction of TPQ_{ox} (0.09 V versus NHE, pH 6.8). In solution, three pK_a values have been detected for the aminoquinol by UV−vis titration and from cyclic voltammetry ($pK_a^1 = 5.88$, $pK_a^2 = 9.59$ and $pK_a^3 = 11.62$).

A species absorbing at 310 nm can also be seen in substrate reduced enzyme under anaerobic conditions (*33*, *37*). The first pK_a for aminoquinol appears to be elevated in the enzyme active site, presumably due to the proximity of the active site base in its ionized form, which can stabilize an adjacent protonated amine at C-5 of TPQ_{red} (analogous to charge stabilization within the substrate and product Schiff base complexes). From UV−vis titration of the aminoquinol and an EPR study of the semiquinone (TPQ_{sq}) that forms from the neutral aminoquinol, the pK_a^1 has been assigned a value of 7.2 in BSAO (*37*) and 6.8 in HPAO (*38*), comparable to a kinetically determined pK_a value for reduction of molecular oxygen (see Oxidative Half Reaction below).

The formation of a protein bound TPQ_{sq} was first observed from anaerobic EPR studies of the substrate reduced form of a variety of CAOs as a function of temperature (*39*). The formation of TPQ_{sq} results from a disproportionation reaction between the active site Cu(II) and the aminoquinol, where a highly variable titer of TPQ_{sq} can be detected, depending on the source of the CAO. It appears that subtle differences in active site structure are sufficient to alter the relative reduction potentials for Cu(II) versus TPQ_{red}. Since electron transfer between Cu(II) and TPQ_{red} was shown to be faster than catalysis, it appeared logical to conclude that Cu(I) would be the site of reactivity for O_2. As shown below, however, the mechanism of O_2 reduction turns out to be contrary to original expectations (see Oxidative Half Reaction).

Rate-Determining Step. The degree of rate limitation by the various steps in the reductive half reaction is dependent on both the source of CAOs and which mutant is being studied. The substrate deuterium isotope effect on k_{cat}/K_m was reported to be 13.5 for BSAO (*30*), while for HPAO, it is reduced to 4.5 (*16*). This suggests that the reductive half reaction is controlled more by C−H bond cleavage in the BSAO reaction. For the D319E mutant of HPAO, no isotope effect was seen on k_{cat}/K_m, and it has been suggested that a conformational change limits the rate (*19*).

OXIDATIVE HALF REACTION (k_{cat}/K_m FOR O_2)

On the basis of the observation of TPQ_{sq} in the substrate reduced form of CAOs under anaerobic conditions, a mechanism (*39*) was proposed involving direct reduction of O_2 by Cu(I) to form Cu(II)−superoxide. Further reduction by TPQ_{sq} would yield Cu(II)−peroxide, and the imino-

Scheme 2: Mechanism for Direct Reduction of Oxygen by TPQ_{red} (*37*)

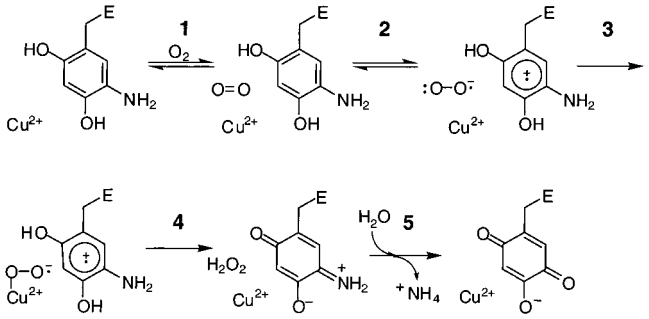

quinone form of TPQ_{ox}. Hydrogen peroxide is then released from the protein and subsequent hydrolysis of the iminoquinone regenerates TPQ_{ox}. Interaction of Cu(I) with O_2 is well known in model systems (*40*) as well as in several protein systems, including dopamine-β-monooxygenase and peptide amidating enzyme (*41*).

Spectrophotometric studies on *Arthrobacter* P1 CAO (*42*) and PSAO (*43*) showed that electron transfer from Cu(II) to TPQ_{red} was too rapid to be rate-limiting. An absence of a solvent viscocity effect on k_{cat}/K_m (O_2) for BSAO ruled out O_2 binding to Cu(I) to form Cu(II)−superoxide as rate-limiting (*37*); the absence of a solvent isotope effect also eliminated peroxide protonation as a rate-limiting step. Finally, rate-limiting peroxide release, where all steps leading up to peroxide release are reversible, was ruled out, as formation of TPQ_{ox} was not biphasic as predicted for this mechanism (*37*). Further, the relative redox potentials for O_2/H_2O_2 ($\epsilon^\circ = 0.28$ V at pH 7 versus NHE) (*44*) and TPQ_{ox}/TPQ_{red} ($\epsilon^\circ = 0.11$ V at pH 7 vs NHE) (*10*), made it unlikely that peroxide could be formed reversibly at the enzyme active site.

The inability to reconcile the experimental results on BSAO with predictions for a Cu(I) mechanism led to a consideration of alternatives and a final proposed mechanism that places the Cu(I)/TPQ_{sq} species off the reaction path (*37*). According to the mechanism in Scheme 2, electrons are transferred directly from TPQ_{red} to O_2 in the catalytic cycle, and O_2 binds initially to a nonmetal site on the enzyme. Following reduction by TPQ_{red}, superoxide can move onto Cu(II), facilitating the transfer of a second electron and two protons from TPQ_{sq}. Analogous to earlier proposed mechanisms, the completion of the oxidative half reaction involves release of bound hydrogen peroxide and hydrolysis of the iminoquinone to release ammonia and regenerate TPQ_{ox}.

O_2 Binding Site. Examination of the X-ray crystal structures for CAOs indicates a dimer interface that is extensively hydrated, with the subunits held together by protruding arms [i.e., the subunits hug each other (*15*, *21*, *23*)]. It has been postulated that O_2, dissolved in the water pocket between the subunits, enters the active site via a discrete channel that leads to a site near, but not on the copper ion (Figure 3).

The exact nature of a nonmetal binding site for O_2 is of considerable interest and not yet fully resolved. Recognizing that O_2 was likely to bind to a hydrophobic portion of the enzyme, a cavity was identified in HPAO which is equatorial to the copper and lined by three hydrophobic amino acids − Y407, L425, and M634 (*37*), Figure 2B. In BSAO, the analogous residues are Tyr, Ala, and Thr. Position 634 in HPAO appears most critical, since M634T confers BSAO-like behavior on HPAO, with regard to the magnitude of k_{cat}/K_m (O_2) (*45*). Systematic change in the side chain at position 634 in HPAO indicates a strong correlation between the size of this residue and the magnitude of k_{cat}/K_m (O_2), with relatively small effects on k_{cat}. Since the latter parameter is limited by cofactor oxidation (see below), it was concluded

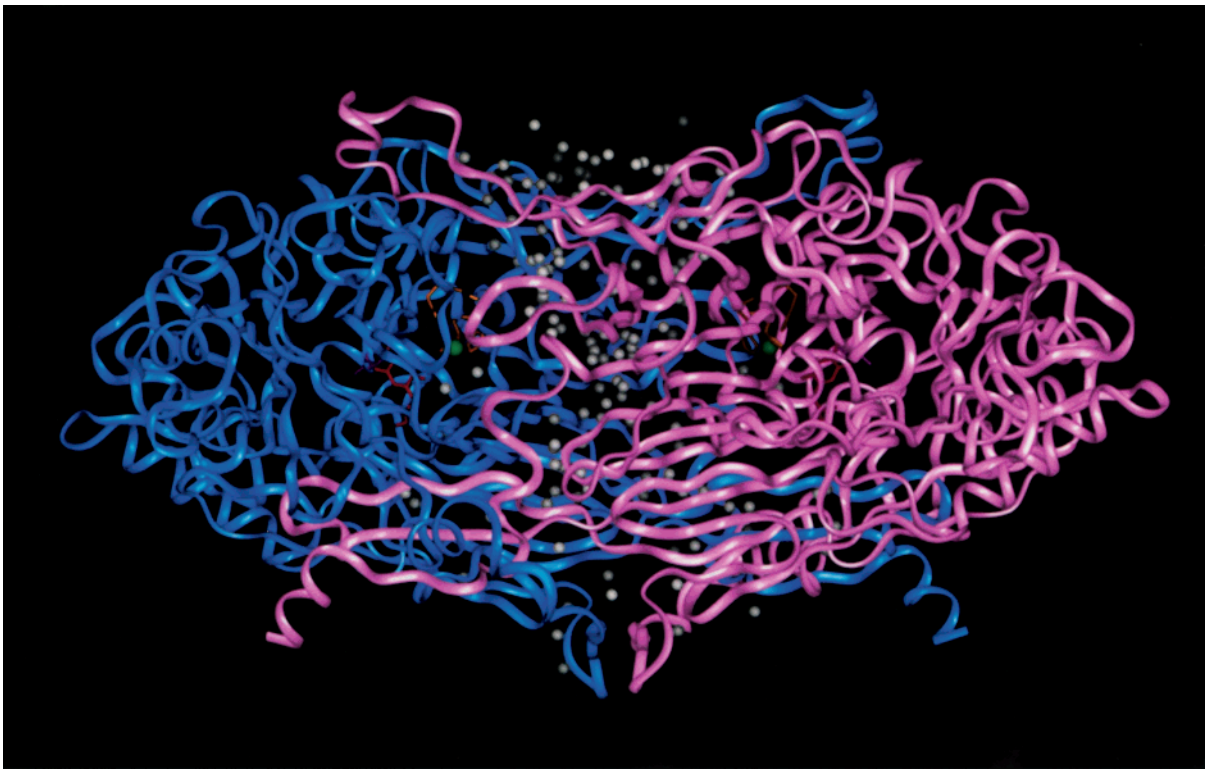

FIGURE 3: Dimer interface showing channel with water molecules (in gray). Subunits are shown in pink and blue. TPQ (in red), D319 (in purple), H458, H456, H624 (in orange), and Cu^{2+} (in light green) are also highlighted.

that residue bulk impacts the strength of O_2 binding (*45*). The precise accommodation of a prebound O_2 for acceptance of an electron from TPQ_{red} has been invoked to explain the finding that N_2 does not compete with O_2 for its binding site (*45*).

Electron Transfer to O_2. Electron transfer from TPQ_{red} to O_2 is the first chemical step in the proposed mechanism, step 2 in Scheme 2 (*37*). Although a two-electron oxidation of an organic molecule by O_2 is spin-forbidden, the chemistry of TPQ model compounds shows that these compounds undergo facile one electron transfer to reduce O_2 (*46*). A second-order rate constant for TPQ_{red} oxidation by O_2 has been determined as 18.6 M^{-1} s^{-1} at pH 7.1 (*46*), which, though slower than enzymatic catalysis, indicates a reasonably efficient direct interaction of TPQ_{red} with molecular oxygen.

The measurement of O-18 kinetic isotope effects reveals a discrimination between O-16 and O-18 with $^{18}[k_{cat}/K_m\ (O_2)] \sim 1.01$, identifying electron transfer to O_2 as the rate-limiting step for both BSAO (*37*) and HPAO (*38*). The reduction in the size of the kinetic isotope effect in relation to a calculated value of 1.03 for conversion of O_2 to superoxide ion (*47*) may have indicated some participation of the active site Cu(II) in stabilizing superoxide ion as it is formed. However, recent studies with both WT-HPAO and a cobalt-substituted form, Co−HPAO, indicate that displacement of metal-bound water occurs after electron transfer (*38*). The size of the measured O-18 kinetic isotope effect is more likely correlated to the ligand reorganization and reaction driving force for oxidation of TPQ_{red} by O_2 (*48*).

The pH profile of k_{cat}/K_m (O_2) indicates two pK_as where catalysis is dependent on the free base forms of two ionizing residues. As noted above (under Reductive Half Reaction), one of the pK_as [7.2 in BSAO (*37*) and 6.8 in HPAO (*38*)] can be assigned with some assurance to the aminoquinol, whose redox potential is reduced upon deprotonation. The second pK_a is likely to be the metal-bound water, since this pK_a is lost upon substitution of Cu(II) by Co(II) (see below), which is expected to raise the pK_a for metal-bound water by several pH units (*49*).

A key feature of the mechanism of Scheme 2 is the lack of a requirement for a valence change at the metal center. This is expected to have the effect of reducing or eliminating the contribution of a metal ligand reorganization term to the rate determining electron transfer. By contrast, the Cu(I) mechanism is critically dependent on the availability of a lower valence form of the active site metal for effective catalysis. Characterization of metal-substituted forms of CAOs is a logical way to distinguish between these mechanisms, and metal replacement studies on the CAOs have been attempted for close to 20 years with mixed results. In an early study (*50*), the Cu(II) of BSAO was replaced with Zn(II), Ni(II), and Co(II). Co(II) was the only ion other than Cu(II) that gave any activity. Recent investigations have reexamined the activity of the Co(II) substituted form of BSAO (*51*), together with the reactivity of Co(II)-substituted BSAO toward various amine substrates (*52*). In all of these studies, the Co(II)-substituted enzyme was found to be significantly less active than for the native, Cu(II)−enzyme.

One troubling aspect of metal replacement studies has been the potential for contaminating copper in metal-substituted CAOs. A somewhat different and more rigorous approach to prepare metal-substituted CAOs was developed for HPAO (*46*). This involves reaction of the Cu(II)-depleted HPAO with the inhibitor, phenylhydrazine. The TPQ−phenylhydrazone complex only forms at subunits that retain metal, thereby inactivating any subunits that have bound residual copper. Subsequent reconstitution of inhibited enzyme eliminates the possibility that measured activity reflects residual Cu(II). The activity of the Co(II)-substituted HPAO prepared in this manner was examined for the first time as a function of O_2 concentration. This study shows that replacement of Cu(II) by Co(II) alters the K_m for O_2 but that saturating O_2 leads to essentially an identical value for k_{cat} at pH 7.1. Since the redox potential for Co(II) to Co(I) is expected to be ca. 800 mV more negative than that for Cu(II) reduction (*53*), this rules out an obligatory reduction of the metal during the oxidative half reaction (*46*).

In a very recent comparison of the properties of WT-HPAO and Co−HPAO, limiting kinetic parameters were obtained at optimal pH values (*38*), showing that k_{cat}/K_m (O_2) is reduced 250-fold for Co−HPAO while k_{cat} is down ca. 3−4-fold. The possibility that the large decrease in k_{cat}/K_m (O_2) for Co−HPAO was due to a change in rate determining step was ruled out by the finding of almost identical properties as for WT-HPAO. These include (i) a lack of dependence on solvent viscosogen, (ii) a small solvent isotope effect, within experimental error of unity, and (iii) a measurable O-18 kinetic isotope effect that is similar to WT-HPAO (*38*).

Perhaps most significantly, the pH dependence of k_{cat}/K_m (O_2) for Co−HPAO shows only a single pK_a value, leading to the conclusion that Co−HPAO functions without ionization of one of the metal-bound waters. This is almost certainly the origin of the large increase in K_m for O_2 with Co−HPAO, which is attributed to an effect of the increased net charge on the metal complex [(+1) for WT-HPAO that contains Cu(II)−OH vs (+2) for Co−HPAO with Co(II)−OH_2] (*38*). Though not previously recognized, the charge at the metal site can be expected to impact the ability of O_2 to bind effectively at the adjacent, hydrophobic site (Figure 2B).

Interaction of Superoxide Anion With Cu(II). Mechanistic studies led to the conclusion that the metal ion of HPAO and superoxide ion interact at some point along the reaction path (*46*), consistent with the X-ray crystallographic study of ECAO that shows binding of product peroxide in close proximity to metal and without an intervening water molecule (*35*). In contrast to Co(II), other divalent metals [Zn(II) and Ni(II)] appear unable to support catalysis, implying that something beyond simple electrostatics is involved in the metal−superoxide interaction, possibly involving charge transfer (*46*). The very low reduction potential for Co(II) versus Cu(II) (*53*, *54*) indicates that charge-transfer complexes between superoxide and these two metal ions would be very different, involving charge donation from superoxide in the case of Cu(II)−enzyme and charge acceptance for the Co(II)−enzyme.

The stage at which the metal-bound water has been lost, opening up a site for superoxide, has been addressed in the more recent study (*38*). From a comparison of the pH dependencies on both k_{cat} and k_{cat}/K_m (O_2) for WT- and Co−HPAO, it has been possible to eliminate mechanisms in which displacement of metal-bound water either precedes O_2 binding to enzyme or occurs concomitant with the first

electron transfer to O_2 (*38*). These results indicate that loss of water follows the first electron transfer step and leads to a positioning of superoxide, most likely in the axial position of metal. The latter is implicated from the structural characterization of reduced ECAO following incubation with O_2, showing oxidized aminoquinol (iminoquinone) and peroxide ion in the axial position (*35*).

In WT-HPAO, the axial water has been suggested to be a proton source in TPQ reduction, leading to copper-hydroxide in the reduced form of enzyme (*41*). The first electron transfer to O_2 from the neutral aminoquinol will significantly perturb the pK_a in the TPQ_{sq} (*37*), such that rapid proton transfer would be expected to proceed from the C-2 oxygen of TPQ_{sq} to the metal hydroxide. The resulting metal-bound water could then undergo the proposed rapid exchange by the superoxide anion.

Proton and Electron Transfer to Copper Superoxide to Form Hydrogen Peroxide. The kinetic properties of k_{cat}/K_m (O_2) do not allow us to address the details of the final chemical steps in O_2 reduction. It is anticipated that the second electron comes from the TPQ_{sq} and that one of the protons required for hydrogen peroxide formation will come from the C-4 oxygen of TPQ_{ox}. The proximity of the active site Tyr (Y305 in HPAO, Figure 2A) to the C-4 oxygen suggested that this residue might be important in a hydrogen bonding network to the copper-hydroperoxide. However, a site-specific mutagenesis experiment to convert this residue to Ala (Y305A in HPAO) indicates an almost identical rate to WT using an aliphatic amine as the substrate (*18*). It is possible that water binding within the "opened up" cavity of the mutant can take on the role of a hydrogen-bonded network normally assumed by the Y305.

Iminoquinone (Formed in Step 4 in Scheme 2). The iminoquinone species was first detected by X-ray crystallography, following incubation of crystals of ECAO with β-phenethylamine (*35*). The UV−vis spectrum of the crystal, when compared with those of model compounds, is consistent with the iminoquinone being in a charge localized form, as the crystal structure shows a short hydrogen bond (2.4 Å) interaction between the C-4 oxygen of the iminoquinone and the conserved Y369 (Y305 in HPAO). In addition, the C-2 oxygen appears directly hydrogen bonded to a dioxygen species that has displaced the axial water of the copper ion and which has been interpreted as hydrogen peroxide (*35*). The release of ammonia from the iminoquinone to solvent may proceed either by hydrolysis to TPQ_{ox} or by a transimination reaction with substrate amine to form the substrate Schiff base (**2** in Scheme 1) (*55*). In model systems, the latter is preferred (*17*).

PROPERTIES OF k_{cat}

The discussion, thus far, has focused on mechanistic steps related to k_{cat}/K_m for O_2 or amine. We now turn our attention to steps contained in k_{cat}. For the two amine oxidases that have been characterized in the greatest detail (BSAO and HPAO), there are obvious differences in rate determining step(s). For BSAO, k_{cat} is approximately 60% rate limited by the reductive half reaction with benzylamine as the substrate (the optimal substrate for BSAO) (*37*). In contrast, k_{cat} in HPAO appears nearly completely limited by steps in the oxidative half reaction with methylamine (the optimal substrate for HPAO) (*16*). For this reason, a discussion of steps limiting k_{cat} is limited to an individual enzyme and cannot be generalized to the entire CAO family.

Steps Limiting k_{cat} in HPAO. The lack of a deuterium isotope effect on k_{cat} with labeled methylamine contrasts sharply with k_{cat}/K_m for amine (*16*) and strongly suggests that k_{cat} in HPAO is controlled by the oxidative half reaction. The pH dependence for k_{cat}/K_m (O_2) [see Oxidative Half Reaction, k_{cat}/K_m (O_2)] increases from pH 6 to 9, with two pK_as, 6.8 and 7.9, and a maximal value above pH 9 (*38*). The pH profile for k_{cat} is bell-shaped with pK_as of 6.1, 7.7, and 8.7 and a maximal value at pH 7.8 (*38*). The kinetic pK_as of 7.9 [k_{cat}/K_m (O_2)] and 7.7 (k_{cat}) have been assigned to ionization of a copper-bound water as a result of comparison of the Co−HPAO to WT-HPAO (*38*). The kinetic pK_a of 6.8 in k_{cat}/K_m (O_2) could also be assigned to the ionization of the protonated TPQ_{red} (*38*), and the pK_a of 6.1 in k_{cat} is likely to reflect the same species. The third pK_a of 8.7 in k_{cat} is unassigned, but is almost certainly related to the fact that the enzyme must be "reset" at the end of the oxidative half reaction by the uptake of a proton, which converts the enzyme to a form that contains copper−water instead of copper−hydroxide. Copper−water is proposed to be one of the proton donors in the reaction of TPQ_{ox} with substrate during the reductive half reaction. This group may be the active site base that has reverted to the elevated pK_a seen in k_{cat}/K_m (amine) (*16*, *30*). Significantly, UV−vis spectroscopic analyses of HPAO indicate that TPQ_{red} is the dominant species that accumulates under steady-state conditions in the presence of excess substrate and O_2 (*19*). Demonstration that electron transfer from TPQ_{red} to O_2 limits k_{cat}/K_m (O_2) comes from the size of the O-18 kinetic isotope effect. Unfortunately, the methodology currently available for measuring the small oxygen isotope effects in O_2-dependent reactions is only suitable to competitive measurements, precluding an analysis of the O-18 isotope effect on k_{cat}.

Steps Limiting k_{cat} in BSAO. From an early study of the pH dependence of the substrate isotope effect, it was concluded that the proton abstraction step of the reductive half reaction significantly limits k_{cat} in BSAO (*30*). The magnitude of the substrate isotope effect, together with the steady-state concentration of TPQ_{ox}, further indicated that the oxidative half reaction limits k_{cat} about 40% and the reductive half reaction limits k_{cat} by 60% (*37*). Analogous to HPAO, it was possible to detect significant levels of TPQ_{red} by UV−vis spectroscopy during steady-state turnover, consistent with electron transfer from TPQ_{red} to bound O_2 as the second major step contributing to k_{cat} for BSAO.

CONCLUSIONS AND FUTURE DIRECTIONS

The TPQ cofactor within the CAOs is a remarkably efficient and precise catalyst. It can catalyze both the two-electron oxidation of an amine substrate via a proton abstraction mechanism and a two-electron reduction of O_2. Throughout these processes, TPQ behaves as a "transducer", storing the two electrons and two protons derived from substrate for delivery to O_2. In many ways, the reductive half reaction resembles pyridoxal phosphate catalysis, in

which a ring structure serves as an electrophilic sink for proton abstraction from substrate (*56*). During the oxidative half reaction, TPQ is more analogous to flavin, supporting reduction of O_2 in the absence of a spin interconversion at the normally unreactive, ground-state triplet O_2 (*57*). Mobility of TPQ appears to be an inherent feature of a cofactor derived from a non-cross-linked tyrosine. In fact, this mobility appears to be a key feature in the biogenesis of TPQ from tyrosine (*8*) but becomes deleterious under conditions of catalytic turnover. In this context, active site mutants that introduce mobility and, as a consequence, an accumulation of intermediates that cannot normally be detected with the wild-type protein have proven extremely useful in confirming mechanistic details. The residues critical for both catalysis and TPQ immobility have been highlighted in Figure 2A for easy reference. The detailed mechanistic studies of the CAOs have raised as many questions as they have answered. One of the fundamental questions is how a single enzyme active site can perform the dual functions of cofactor biogenesis and catalysis. Comparison of the zinc-containing precursor to the mature, copper form of HPAO by X-ray crystallography shows that the bulk of the protein is unaltered, with only subtle features undergoing detectable change (*58*). This challenging topic has begun to be addressed in separate, recent reviews (*59*−*61*). The CAOs are known to vary a great deal in their preferred substrate specificity (*5*, *16*, *62*, *63*). The structural origin of this specificity is currently unknown and will require structural comparisons among highly homologous isozymes that have a preference for different amines (e.g., aliphatic versus aromatic amine substrates). The reductive half reaction of BSAO has been documented to catalyze the C−H cleavage via hydrogen tunneling (*32*). Analogous to other enzyme systems with a significant H-tunneling component, it should be very informative to examine the role of active site residues in H-transfer, in particular, which interactions between substrate and enzyme play a role in modulating the barrier shape for hydrogen transfer. The oxidative half reaction of the CAOs has been full of surprises. The implication of a nonmetal, hydrophobic pocket to bind dioxygen is provocative and in need of greater clarification. For example, given the composition of the atmosphere, 20% O_2 and 80% N_2, how does an enzyme accommodate dioxygen in the presence of an excess of dinitrogen? Given the absence of a formal valence change for the active site cupric ion in the CAOs during catalytic turnover and the viability of cobaltous, but not the zinc-containing enzyme, it becomes especially compelling to define the precise catalytic role of the active site metal in charge stabilization, spin interconversion, and hydrogen bonding/proton transfer from the metal-bound water molecules. One aspect of the CAOs that has never been adequately resolved is the possible role of cooperativity among the subunits. Examination of the dimeric structures of numerous CAOs indicates the use of side chains from one subunit in defining the catalytic site on the opposing subunit. Well-designed site-directed mutagenesis studies may hold the key to the impact of subunit interactions on catalytic turnover and catalysis. As discussed under Oxidative Half Reaction, it has been postulated that O_2 reaches the active site of HPAO via a specific channel in the protein. This raises the general question of how O_2 binds to proteins, i.e., whether this occurs in a nonspecific manner via hydrophobic patches on the proteins, as has been generally believed, or whether directed pathways have evolved for "shepherding" dioxygen from bulk solvent to the active site.

As the above partial list indicates, there is much more work to be done.

REFERENCES

1. Janes, S. M., Mu, D., Wemmer, D., Smith, A. J., Kaur, S., Maltby, D., Burlingame, A. L., and Klinman, J. P. (1990) *Science 248*, 981−987.
2. Wang, S. X., Mure, M., Medzihradszky, K. F., Burlingame, A. L., Brown, D. E., Dooley, D. M., Smith, A. J., Kagan, H. M., and Klinman, J. P. (1996) *Science 273*, 1078−1084.
3. McIntire, W. S., Wemmer, D. E., Christoserdov, A., and Lidstrom, M. E. (1991) *Science 252*, 817−824.
4. Vandenberghe, I., Kim, J. K., Devreese, B., Hacisalihoglu, A., Iwabuki, H., Okajima, T., Kuroda, S., Adachi, O., Jongejan, J. A., Duine, J. A., Tanizawa, K., and Van Beeumen, J. (2001) *J. Biol. Chem. 276*, 42923−42931.
5. Matsuzaki, R., Fukui, T., Sato, H., Ozaki, Y., and Tanizawa, K. (1994) *Febs Lett. 351*, 360−364.
6. Cai, D., and Klinman, J. P. (1994) *J. Biol. Chem. 269*, 32039−32042.
7. Dove, J. E., Schwartz, B., Williams, N. K., and Klinman, J. P. (2000) *Biochemistry 39*, 3690−3698.
8. Schwartz, B., Dove, J. E., and Klinman, J. P. (2000) *Biochemistry 39*, 3699−3707.
9. Klinman, J. P. (1996) *J. Biol. Chem. 271*, 27189−27192.
10. Mure, M., and Klinman, J. P. (1993) *J. Am. Chem. Soc. 115*, 7117−7127.
11. Kishishita, S.-I. (1997), M.S. Thesis, ISSR, Osaka University, Osaka, Japan.
12. Moenneloccoz, P., Nakamura, N., Steinebach, V., Duine, J. A., Mure, M., Klinman, J. P., and Sandersloehr, J. (1995) *Biochemistry 34*, 7020−7026.
13. Mure, M., and Klinman, J. P. (1995) *J. Am. Chem. Soc. 117*, 8698−8706.
14. Murray, J. M., Kurtis, C. R., Tambyrajah, W., Saysell, C. G., Wilmot, C. M., Parsons, M. R., Phillips, S. E. V., Knowles, P. F., and McPherson, M. J. (2001) *Biochemistry 40*, 12808−12818.
15. Li, R., Klinman, J. P., and Mathews, F. S. (1998) *Structure 6*, 293−307.
16. Hevel, J. M., Mills, S. A., and Klinman, J. P. (1999) *Biochemistry 38*, 3683−3693.
17. Mure, M., and Klinman, J. P. (1995) *J. Am. Chem. Soc. 117*, 8707−8718.
18. Nakamura, N., Moënne-Loccoz, P., Tanizawa, K., Mure, M., Suzuki, S., Klinman, J. P., and Sanders-Loehr, J. (1997) *Biochemistry 36*, 11479−86.
19. Plastino, J., Green, E. L., Sanders-Loehr, J., and Klinman, J. P. (1999) *Biochemistry 38*, 8204−8216.
20. Schwartz, B., Green, E. L., Sanders-Loehr, J., and Klinman, J. P. (1998) *Biochemistry 37*, 16591−16600.
21. Parsons, M. R., Convery, M. A., Wilmot, C. M., Yadav, K. D., Blakeley, V., Corner, A. S., Phillips, S. E., McPherson, M. J., and Knowles, P. F. (1995) *Structure 3*, 1171−1184.
22. Kumar, V., Dooley, D. M., Freeman, H. C., Guss, J. M., Harvey, I., McGuirl, M. A., Wilce, M. C., and Zubak, V. M. (1996) *Structure 4*, 943−955.
23. Wilce, M. C., Dooley, D. M., Freeman, H. C., Guss, J. M., Matsunami, H., McIntire, W. S., Ruggiero, C. E., Tanizawa, K., and Yamaguchi, H. (1997) *Biochemistry 36*, 16116−16133.
24. Murray, J. M., Saysell, C. G., Wilmot, C. M., Tambyrajah, W. S., Jaeger, J., Knowles, P. F., Phillips, S. E., and McPherson, M. J. (1999) *Biochemistry 38*, 8217−8227.
25. Green, E. L., Nakamura, N., Dooley, D. M., Klinman, J. P., and Sanders-Loehr, J. (2002) *Biochemistry 41*, 687−696.
26. Wilmot, C. M., Murray, J. M., Alton, G., Parsons, M. R., Convery, M. A., Blakeley, V., Corner, A. S., Palcic, M. M., Knowles, P. F., McPherson, M. J., and Phillips, S. E. (1997) *Biochemistry 36*, 1608−1620.
27. Nakamura, N., Matsuzaki, R., Choi, Y. H., Tanizawa, K., and Sanders-Loehr, J. (1996) *J. Biol. Chem. 271*, 4718−4724.
28. Hartmann, C., and Klinman, J. P. (1987) *J. Biol. Chem. 262*, 962−965.

29. Hartmann, C., and Klinman, J. P. (1990) *Febs Lett. 261*, 441−444.
30. Farnum, M., Palcic, M., and Klinman, J. P. (1986) *Biochemistry 25*, 1898−904.
31. Palcic, M. M., and Klinman, J. P. (1983) *Biochemistry 22*, 5957−5966.
32. Grant, K. L., and Klinman, J. P. (1989) *Biochemistry 28*, 6597−6605.
33. Hartmann, C., Brzovic, P., and Klinman, J. P. (1993) *Biochemistry 32*, 2234−2241.
34. Cai, D. Y., Dove, J., Nakamura, N., SandersLoehr, J., and Klinman, J. P. (1997) *Biochemistry 36*, 11472−11478.
35. Wilmot, C. M., Hajdu, J., McPherson, M. J., Knowles, P. F., and Phillips, S. E. (1999) *Science 286*, 1724−1728.
36. Prabhakar, R., and Siegbahn, P. E. M. (2001) *J. Phys. Chem. B 105*, 4400−4408.
37. Su, Q. J., and Klinman, J. P. (1998) *Biochemistry 37*, 12513−12525.
38. Mills, S. A., Goto, Y., Su, Q., Plastino, J., and Klinman, J. P. (2002) *Biochemistry*, submitted.
39. Dooley, D. M., McGuirl, M. A., Brown, D. E., Turowski, P. N., McIntire, W. S., and Knowles, P. F. (1991) *Nature 349*, 262−264.
40. Karlin, K. D., Kaderli, S., and Zuberbuhler, A. D. (1997) *Acc. Chem. Res. 30*, 139−147.
41. Klinman, J. P. (1996) *Chem. Rev. 96*, 2541−2561.
42. Dooley, D. M., and Brown, D. E. (1996) *J. Biol. Inorg. Chem. 1*, 205−209.
43. Turowski, P. N., Mcguirl, M. A., and Dooley, D. M. (1993) *J. Biol. Chem. 268*, 17680−17682.
44. Sawyer (1991) *Oxygen Chemistry*, Oxford University Press, New York.
45. Goto, Y., and Klinman, J. P. (2002) Personal communication.
46. Mills, S. A., and Klinman, J. P. (2000) *J. Am. Chem. Soc. 122*, 9897−9904.
47. Tian, G. C., and Klinman, J. P. (1993) *J. Am. Chem. Soc. 115*, 8891−8897.
48. Roth, J., and Klinman, J. P. (2002) Personal communication.
49. Richens, D. T. (1997) *The Chemistry of Aqua Ions*, John Wiley & Sons, New York.
50. Suzuki, S., Sakurai, T., Nakahara, A., Manabe, T., and Okuyama, T. (1983) *Biochemistry 22*, 1630−1635.
51. Agostinelli, E., De Matteis, G., Mondovi, B., and Morpurgo, L. (1998) *Biochem. J. 330*, 383−387.
52. De Matteis, G., Agostinelli, E., Mondovi, B., and Morpurgo, L. (1999) *J. Biol. Inorg. Chem. 4*, 348−353.
53. Drummond, J. T., and Matthews, R. G. (1994) *Biochemistry 33*, 3732−3741.
54. Karlin, K. D., and Gultneh, Y. (1987) *Prog. Inorg. Chem. 35*, 219−327.
55. Janes, S. M., and Klinman, J. P. (1991) *Biochemistry 30*, 4599−4605.
56. Frey, P. A., Petrovich, R. M., Song, K. B., and Han, O. (1991) *Proc. 8th Int. Symp. Vitam. B6 Carbonyl Catal.*, 357−363.
57. Miura, R. (2001) in *Chem. Rec.* pp 183−194.
58. Chen, Z. W., Schwartz, B., Williams, N. K., Li, R. B., Klinman, J. P., and Mathews, F. S. (2000) *Biochemistry 39*, 9709−9717.
59. Dooley, D. M. (1999) *J. Biol. Inorg. Chem. 4*, 1−11.
60. Dove, J. E., and Klinman, J. P. (2001) *Adv. Protein Chem. 58*, 141−174.
61. Klinman, J. P. (2001) *Proc. Nat. Acad. Sci. U.S.A. 98*, 14766−14768.
62. Choi, Y. H., Matsuzaki, R., Fukui, T., Shimizu, E., Yorifuji, T., Sato, H., Ozaki, Y., and Tanizawa, K. (1995) *J. Biol. Chem. 270*, 4712−4720.
63. Kucha, J. A., and Dooley, D. M. (2001) *J. Inorg. Biochem. 83*, 193−204.
64. McGuirl, M. A., McCahon, C. D., McKeown, K. A., and Dooley, D. M. (1994) *Plant Physiol. 106*, 1205−1211.
65. Cai, D., and Klinman, J. P. (1994) *Biochemistry 33*, 7647−7653.

BI020246B